Desalination and Water Treatment
www.deswater.com
doi: 10.1080/19443994.2012.749023

51 (2013) 3164–3178
April

Taylor & Francis
Taylor & Francis Group

Lanthanides as environmentally friendly corrosion inhibitors of iron in 3.5% NaCl solution

A.S. Fouda[a,*], H. Megahed[b], D.M. Ead[a]

[a]*Department of Chemistry, Faculty of Science, El-Mansoura University, El-Mansoura-35516, Egypt*
Tel. +2 050 2365730; Fax: +2 050 2446254; email: asfouda@mans.edu.eg
[b]*Department of Chemistry, Faculty of Science, Benha University, Benha, Egypt*

Received 10 August 2011; Accepted 30 September 2012

ABSTRACT

Lanthanides have been evaluated as new corrosion inhibitors for the corrosion of iron in 3.5% NaCl solutions using electrochemical techniques [potentiodynamic polarization, electrochemical impedance spectroscopy, and electrochemical frequency modulation]. The adsorption of lanthanides on iron surface was found to be of neither a typical physisorption nor a typical chemisorption mode. Increase in temperature increases corrosion rate but decreases inhibition efficiency. The thermodynamic functions of activation have been evaluated. The polarization measurements indicated that the inhibitors are of mixed type. The adsorption of these compounds was found to obey Langmuir's adsorption isotherm. The analysis of scanning electron microscopy and electron dispersion X-Ray confirmed the formation of precipitates of lanthanides on iron surface, which reduced the overall corrosion reaction.

Keywords: Corrosion; Inhibition; Iron; NaCl; Lanthanides; EIS; EFM

1. Introduction

Iron and steel are used in most industries because of its low cost and availability for manufacture of reaction vessels such as cooling towers reservoirs, pipelines, boilers, drums heat exchangers, tanks, etc. Iron and steel structures are highly susceptible to corrosion and their protection costs billions of dollars annually. Various additives are used to protect iron and its alloy against corrosive attack. It is well known that lanthanide ions form insoluble hydroxides which enable them to be used as cathodic inhibitors. Lanthanides have a low toxicity and their ingestion or inhalation has not been considered harmful to health [1], whilst the toxic effects of their oxides are similar to those produced by sodium chloride. Furthermore, lanthanides can be considered as economically competitive products [2] because, as elements, some of them are relatively abundant in nature. Cerium, for instance, is as plentiful as copper [3]. Production of lanthanides has shown a continuous increase in recent years. Taking all these facts into account, it is reasonable to use this family of compounds as save corrosion inhibitors. There are several papers in the literature dealing with the use of lanthanides as corrosion inhibitors for several metals and alloys such as zinc [4–6], mild steels [7], and stainless steels [8–14]. Several researches were found in the literature about the use of inhibitors for metals and alloys in seawater [15–17].

The present work has been designated to evaluate the effect of lanthanides on the corrosion inhibition of iron in 3.5% NaCl solution. Electrochemical techniques such as potentiodynamic polarization, electrochemical impedance spectroscopy (EIS) and electrochemical frequency modulation (EFM) have been employed to

*Corresponding author.

study the corrosion rate and inhibition efficiency. Activation and thermodynamic parameters were effectively used to characterize the inhibition mechanism of the adsorption process.

2. Experimental method

The working electrode was prepared from high purity (99.879%) iron wire. This iron wire was fixed to borosilicate glass tube with epoxy resin. Before being used, the electrode surface was abraded with different grade emery papers (from 120 to 1,200 grit) until it appeared free from scratching and other defects. Then, degreased with acetone and finally washed with double distilled water before they were inserted into the test solution.

All chemicals used for preparing the test solutions were of analytical grade and the experiments were carried out at room temperature, 25 ± 1°C using Lab companion circulator thermostat model CW-05GL. The aggressive and inhibitors solutions were made from double distilled water.

Measurements were made in a three-compartment cell with a platinum foil auxiliary electrode and a saturated calomel reference electrode (SCE) was used. All experiments were repeated at minimum of two times.

Potentiodynamic measurements were carried out, after immersion the electrode for 30 min in the test solution to attain steady state. For polarization measurements potential was scanned from −800 to +800 mV (relative to SCE) at a scan rate of 1 mV s^{-1}. The EIS tests were performed at corrosion potentials (E_{corr}) over a frequency range of 100 kHz–0.2 Hz with an ac wave of ±5 mV peak-to-peak after immersion the electrode for 30 minutes in the test solutions. All the electrochemical experiments were carried out using Potentiostat/Galvanostat/ZRA analyzer (Gamry PCI 300/4). A personal computer with DC 105 software for potentiodynamic polarization, EIS300 software for impedance, EFM140 for electrochemical frequency modulation and Echem. Analyst 5.21 was used for data fitting and calculating.

3. Results and discussion

3.1. Potentiodynamic polarization measurements

The values of corrosion potential (E_{corr}), corrosion current density (j_{corr}), and anodic and cathodic Tafel slopes (β_a and β_c) can be evaluated from anodic and cathodic regions of Tafel plots. The linear Tafel segments of anodic and cathodic curves were extrapolated to corrosion potential to obtain corrosion current densities (j_{corr}).

The inhibition efficiency, η, and the surface coverage, θ, were evaluated from the measured (j_{corr}) values using the relationship [18]:

$$\eta\ (\%) = \theta \times 100 = [(j'_{corr} - j_{corr})/j'_{corr}] \times 100 \quad (1)$$

where j'_{corr} and j_{corr} are values of corrosion current density in the absence and presence of inhibitor, respectively.

Potentiodynamic polarization curves for the corrosion of iron in 3.5% NaCl in the absence and presence of different concentrations of $SmCl_3$ at 25°C are presented in Fig. 1 as an example. Similar curves were obtained for $LaCl_3$ and $CeCl_3$ (not shown). From Fig. 1, it is clear that both the cathodic and the anodic reactions are inhibited and the inhibition increases as the inhibitor concentration increases, but the cathode is more polarized. The values of various electrochemical parameters derived from Tafel polarization of all inhibitors are given in Table 1. The results of Table 1 indicate that, there was no definite trend observed in the E_{corr} values in the presence of investigated lanthanides. In the present study, shift in E_{corr} values is in the range of 40 mV suggesting that all inhibitors act as mixed type [19]. Also, the change in β_a and β_c values (Table 1) indicates that adsorption of investigated lanthanides affect the mechanism of anodic dissolution as well as cathodic hydrogen evolution. This, confirm that these investigated lanthanides act as mixed-type inhibitors, but predominantly cathodic inhibitors [20]. It is seen (Table 1) that the inhibition efficiency of investigated lanthanides shows the following order:

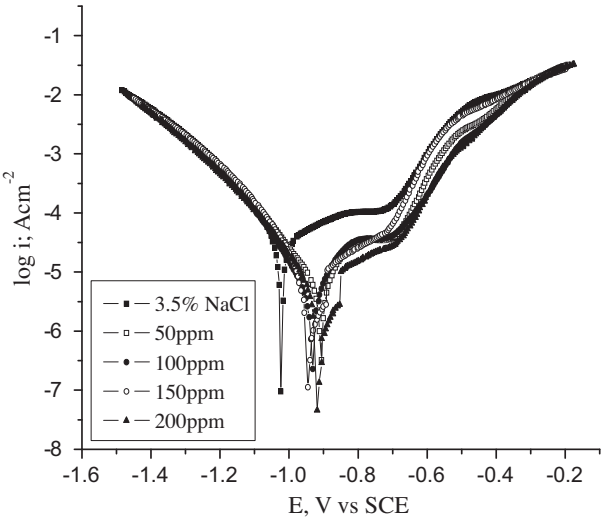

Fig. 1. Potentiodynamic polarization curves for the corrosion of iron in 3.5% NaCl in the absence and presence of different concentrations of $SmCl_3$ at 25°C.

Table 1
Effect of lanthanide chlorides concentrations on the free corrosion potential (E_{corr}), corrosion current density (j_{orr}), Tafel slopes (β_c, β_a), degree of surface coverage (θ), and inhibition percent (η%) for corrosion of iron in 3.5% NaCl at 25°C

Inh.	[Inh.] (ppm)	$-E_{corr}$ (mV)	j_{corr} ($\mu A\,cm^{-2}$)	β_c ($mV\,dec^{-1}$)	β_a ($mV\,dec^{-1}$)	$R_p \times 10^3$ ($\Omega\,cm)^2$	C.R. ($mm\,y^{-1}$)	θ	η,%
La	Blank	1,004	23.49	157	308	1.926	0.273	–	–
	50	978	11.92	158	282	3.691	0.138	0.492	49.2
	100	985	11.91	148	283	3.544	0.138	0.493	49.3
	150	967	10.85	151	278	3.910	0.126	0.538	53.8
	200	973	9.543	147	271	4.333	0.111	0.594	59.4
Ce	50	986	10.93	146	286	3.850	0.127	0.535	53.5
	100	966	10.99	151	281	3.887	0.128	0.532	53.2
	150	973	8.694	146	265	4.708	0.101	0.630	63.0
	200	962	7.924	144	270	5.148	0.092	0.663	66.3
Sm	50	908	10.59	179	255	4.317	0.123	0.549	54.9
	100	932	8.501	166	250	5.090	0.099	0.638	63.8
	150	948	4.375	143	243	8.926	0.051	0.814	81.4
	200	918	2.667	142	214	1.390	0.031	0.887	88.7

$SmCl_3 > CeCl_3 > LaCl_3$. Increase in the inhibition efficiency with increasing concentration of all lanthanides studied reveals that the inhibition action are due to adsorption on iron surface and the adsorption is known to depend on the chemical structure of the inhibitors.

The polarization resistance (R_p) values are apparent to increase with increasing inhibitor concentration (Table 1).

3.2. Adsorption isotherm

Basic information on the interaction between inhibitors and metal surface can be provided using the adsorption isotherms [21]. In order to obtain the adsorption isotherm, the degree of surface coverage, θ, for different concentrations of inhibitor in 3.5% NaCl solution has been evaluated from potentiodynamic polarization (Table 1).

Attempts were made to fit these θ values to various isotherm indicating Frumkin, Langmuir, Temkin, etc. The best fit was obtained with Langmuir isotherm (Fig. 2). According to this isotherm, θ is related to inhibitor concentration by the equation [18]:

$$C/\theta = 1/K_{ads} + C \quad (2)$$

where K_{ads} is the equilibrium constant of the adsorption process and C is the concentration of the inhibitor. For pure iron, the plot of C/θ against (C) gave a straight line with a correlation coefficient > 0.98, and with almost higher slope than unity (1.1 in case of La and Ce) as shown in Fig. 2. This indicates the presence of interactions among the adsorbed species adjacent to each other. This behavior suggests that the lanthanides adsorbed onto the iron surface following the Langmuir adsorption isotherm.

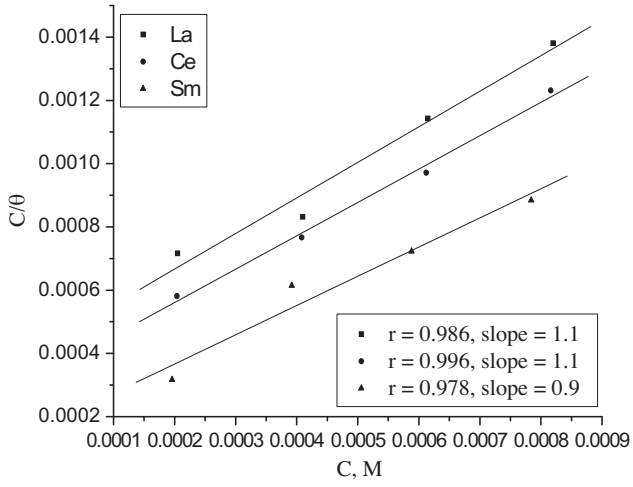

Fig. 2. Curve fitting for iron in 3.5% NaCl in the presence of different concentrations of lanthanides chlorides to Langmuir adsorption isotherm at 25°C.

The K_{ads} values can be calculated from the intercept lines on the C/θ-axis. This value is also related to the standard free energy of adsorption (ΔG°_{ads}) by the following equation:

$$\Delta G^{\circ}_{ads} = -RT\ln(55.5K_{ads}) \quad (3)$$

where R is the universal gas constant and T is the absolute temperature. The value of 55.5 is the concentration

Table 2
Equilibrium constant (K_{ads}), free energy of binding (ΔG°_{ads}), number of active sites ($1/y$), and Langmuir slope of lanthanides for iron in 3.5% NaCl solution

Inh.	Kinetic model			Langmuir isotherm	
	$1/y$	$K_{ads} \times 10^{-3}\,M^{-1}$	$-\Delta G^{\circ}_{ads}$ (kJ mol^{-1})	$K_{ads} \times 10^{-3}\,M^{-1}$	$-\Delta G^{\circ}_{ads}$ (kJ mol^{-1})
$LaCl_3$	1.2	3.4	30.1	2.3	29.1
$CeCl_3$	1.4	5.5	31.3	2.9	29.7
$SmCl_3$	1.5	5.1	31.1	5.5	31.3

of water in bulk solution in mol l^{-1}. The values of K_{ads} and ΔG°_{ads} for lanthanides in 3.5% NaCl solution are given in Table 2. The negative sign of ΔG°_{ads}. indicates that investigated lanthanides are spontaneously adsorbed on iron surface. Generally, the magnitude of ΔG°_{ads} is around -20 kJ mol^{-1} or less negative, which can be assumed that an electrostatic interaction exists between the inhibitor and the charged metal surface (i.e. physisorption). Standard free energy of adsorption (ΔG°_{ads}) around -40 kJ mol^{-1} or more negative indicated that a charge sharing or transferring from organic species to the metal surface occurs to form a coordinate type of bond (i.e. chemisorption) [22]. It should be mentioned that the higher values of K_{ads} and ΔG°_{ads} refer to a higher adsorptive and thus a higher inhibiting effect. The ΔG°_{ads} values obtained for the studied compounds on iron surface in 3.5% NaCl ranged from -29.1 to -31.3 kJ mol^{-1}, indicating both physical and chemical adsorption [23].

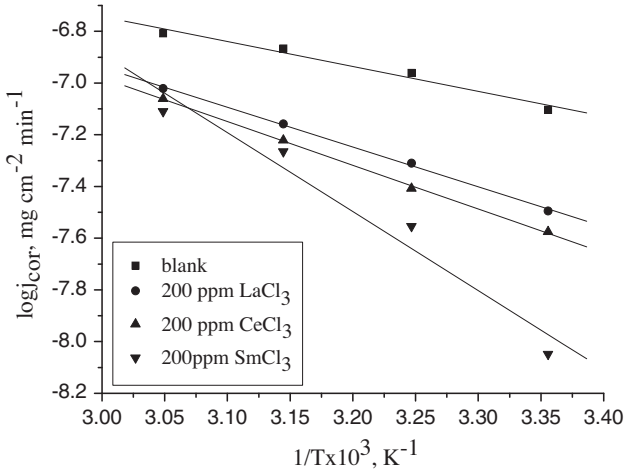

Fig. 4. Arrhenius plots $\log j_{corr}$ vs. $1/T$ for iron in 3.5% NaCl in absence and presence of 200 ppm of lanthanides chlorides.

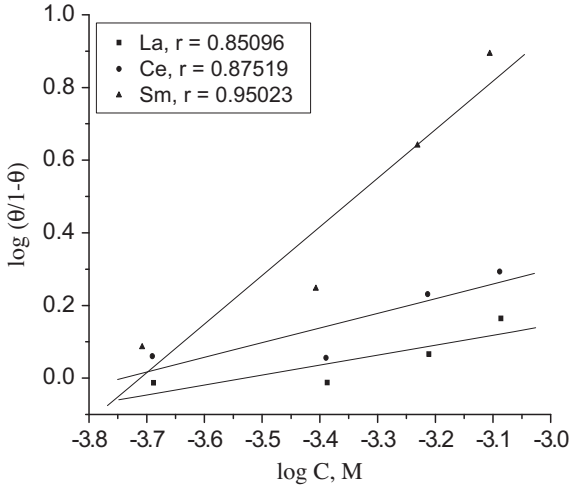

Fig. 3. Curve fitting for iron in 3.5% NaCl in the presence of different concentrations of lanthanides chlorides to El Awady et al model at 25°C.

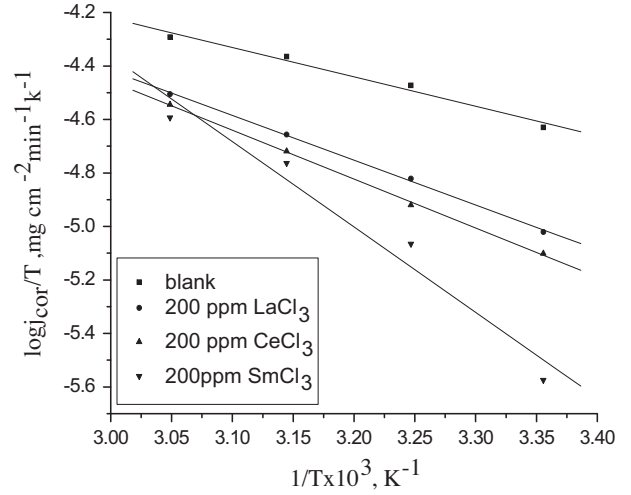

Fig. 5. Log j_{corr}/T vs. $1/T$ for iron in 3.5% NaCl in the absence and presence of 200 ppm of the lanthanides.

Table 3
Effect of temperature on the free corrosion potential (E_{corr}), corrosion current density (j_{corr}), Tafel slopes (β_c, β_a), inhibition percent (η%), and degree of surface coverage (θ) of Fe in 3.5% NaCl in the absence and presence of 200 ppm of the lanthanides chlorides

Temp°C	Inh.	$-E_{corr}$ (mV)	j_{corr} (μ A cm^{-2})	β_c (mV dec^{-1})	β_a (mV dec^{-1})	$R_p \times 10^3$ (Ω cm^2)	CR	θ	η (%)
35	Blank	929.6	33.67	207	271	1.514	0.391	–	–
	La	943.1	15.10	155	271	2.840	0.175	0.552	55.2
	Ce	952.8	12.03	156	274	3.586	0.140	0.643	64.3
	Sm	949.4	8.616	153	257	4.836	0.100	0.744	74.4
45	Blank	957.4	43.21	189	274	1.123	0.502	–	–
	La	927.3	22.08	174	263	2.056	0.256	0.481	48.1
	Ce	927.7	19.11	178	264	2.413	0.222	0.558	55.8
	Sm	949.1	17.27	166	268	2.574	0.200	0.60	60.00
55	Blank	923.2	51.05	210	267	0.9997	0.593	–	–
	La	888.4	31.26	196	257	1.543	0.363	0.388	38.8
	Ce	967.0	28.52	170	270	1.588	0.331	0.441	44.1
	Sm	907.5	25.51	191	247	1.832	0.296	0.50	50.0

Table 4
Thermodynamic activation parameters for dissolution of iron in 3.5% NaCl in the absence and presence of 200 ppm of lanthanide chlorides

Inhibitor	Thermodynamic activation parameter		
	E_a^* (kJ mol^{-1})	ΔH^* (kJ mol^{-1})	$-\Delta S^*$ (J mol^{-1} K^{-1})
3.5% $NaCl_3$	21.0	18.9	271.4
$LaCl_3$	32.1	29.5	242.1
$CeCl_3$	35.0	32.4	234.1
$SmCl_3$	61.1	58.5	154.0

On the other hand, it is found that the kinetic–thermodynamic model of El-Awady et al [24]:

$$\log \theta/(1-\theta) = \log K' + y \log C \quad (4)$$

is valid to operate the present adsorption data. The equilibrium constant of adsorption $K = K'^{(1/y)}$, where $1/y$ is the number of the surface active sites occupied by one inhibitor molecule and C is the bulk concentration of the inhibitor. Plotting $\log \theta/(1-\theta)$ against $\log C$ at 25°C is given in Fig. 3, where straight line relationships were obtained suggesting the validity of this model for all cases studied. The calculated values of $1/y$, K_{ads} and ΔG°_{ads} are given in Table 2. It is noting

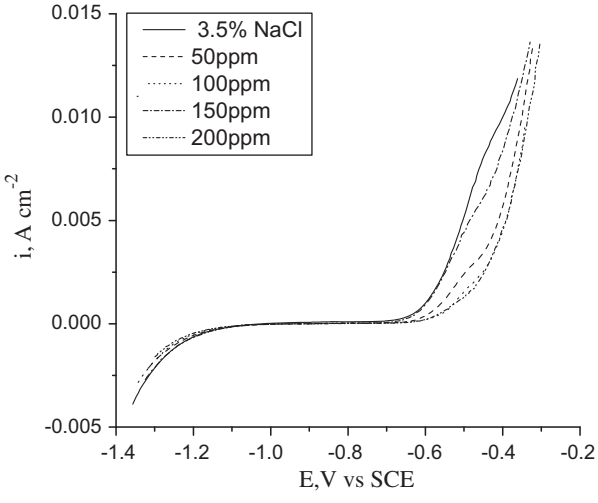

Fig. 6. Potentiodynamic anodic curves for iron in 3.5% NaCl in the absence and presence of different concentrations of $SmCl_3$ at 25°C.

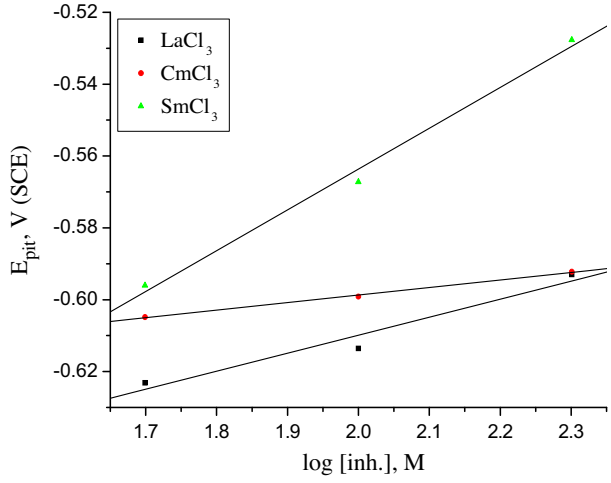

Fig. 7. Pitting potential (E_{pit}) as a function of lanthanide concentrations for iron in 3.5% NaCl. solution.

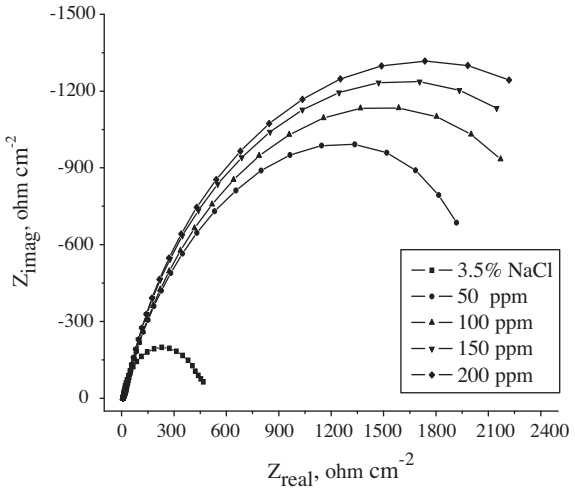

Fig. 8. Nyquist plots for corrosion of iron in 3.5% NaCl in the absence and presence of different concentrations of $SmCl_3$ at 25°C.

that the values of $1/y$ is around unity, this means that the given inhibitor molecules will occupy one active site. In general, the values of ΔG°_{ads} obtained from El-Awady et al model are comparable with those obtained from Langmuir isotherm.

3.3. Effect of temperature

The influence of temperature on the corrosion rate of iron in 3.5% NaCl in the absence and presence of 200 ppm of the lanthanides was investigated by the potentiodynamic polarization technique in temperature range (25–55°C). The effect of increasing temperature on the inhibition efficiency values is listed in Table 3. The results revealed that, on increasing temperature there is an increase of corrosion rate while inhibition efficiency decreases for all compounds used.

Plots of logarithm of corrosion rate ($\log k$) with reciprocal of absolute temperature ($1/T$) for iron 3.5% NaCl in the absence and presence of 200 ppm of the lanthanides are shown in Fig. 4. All the linear regression coefficients are close to 1, indicating that corrosion of iron in 3.5% NaCl can be explained using the kinetic model. As shown from this figure, straight lines with slope $-E^{*}_{a}/2.303R$ and intercept of A were obtained according to Arrhenius-type equation:

$$k = A \exp\left(-E^{*}_{a} / RT\right), \tag{5}$$

where k is the corrosion rate, A is a constant depends on a metal type, and electrolyte E^{*}_{a} is the apparent activation energy.

Plots of log (corrosion rate/T) vs. $1/T$ for iron in 3.5% NaCl in the absence and presence of 200 ppm of the lanthanides are shown in Fig. 5. As shown from this figure, straight lines with slope of $(-\Delta H^{*}/2.303R)$ and intercept of $(\log(R/Nh) + \Delta S^{*}/2.303R)$ were obtained according to transition state equation:

$$\text{Rate} = RT/Nh \exp(\Delta S^{*}/R) \exp\left(-\Delta H^{*}/RT\right) \tag{6}$$

where h is Planck's constant, N is Avogadro's number, ΔH^{*} is the activation enthalpy, and ΔS^{*} is the activation entropy.

Table 5
Impedance data for corrosion of iron in 3.5% NaCl in the absence and presence of different concentrations of lanthanides chlorides compounds at 25°C

Inh.	[Inh.] (ppm)	$C_{dl,}$ (μF cm^{-2})	$R_{ct,}$ (Ω cm^2)	θ	η (%)
$LaCl_3$	Blank	498.6	439	–	–
	50	421.3	1,181	0.628	62.8
	100	406.0	1,420	0.691	69.1
	150	363.4	1,613	0.728	72.8
	200	321.3	1806	0.753	75.3
$CeCl_3$	50	375.1	1,429	0.693	69.3
	100	349.9	1,706	0.743	74.3
	150	306.7	1,793	0.755	75.5
	200	249.5	1929	0.772	77.2
$SmCl_3$	50	343.6	1,597	0.725	72.5
	100	312.5	1,765	0.751	75.1
	150	284.2	1972	0.777	77.7
	200	227.3	2068	0.788	78.8

The calculated values of the apparent activation energy, E_a^*, activation enthalpies, ΔH^*, and activation entropies, ΔS^*, are given in Table 4. These values indicate that the presence of the additives increases the activation energy, E_a^*, and the activation enthalpy, ΔH^*, and decreases the activation entropy, ΔS^*, for the corrosion process. The increase in the activation energy indicating a strong adsorption of the inhibitor molecules on iron surface and indicates the energy barrier caused by the adsorption of the additive molecules on aluminum surface. The increase in the activation enthalpy (ΔH^*) in the presence of the inhibitors implies that the addition of the inhibitors to the acid solution increases the height of the energy barrier of the corrosion reaction to an extent depends on the type and concentration of the present inhibitor. The entropy of activation (ΔS^*) in the blank and inhibited solutions is large and negative indicating that the activated complex represents association rather than dissociation step [25].

The order of decreasing inhibition efficiency of the investigated compounds as gathered from the increase in E_a^* and ΔH_{ads}^* values and decrease in ΔS_{ads}^* values is as follows: $SmCl_3 > CeCl_3 > LaCl_3$

3.4. Pitting corrosion

The effect of adding different concentrations of the lanthanides on the pitting corrosion behavior of iron in 3.5% NaCl solution was investigated by potentiodynamic polarization measurements. Fig. 6 shows these effects for different concentrations of $SmCl_3$ as an example. It is observed that the addition of different concentrations of $SmCl_3$ to 3.5% NaCl solution increases the breakdown potential towards more positive values, i.e. inhibits pitting corrosion of the iron. Fig. 7 shows the relation between pitting potential; E_{pit} and the inhibitors concentrations, a straight line obtained according to the following equation:

$$E_{pit} = a' + b' \log [inh] \quad (7)$$

Symbols a' and b' are constants. The increase of the inhibitors concentration increases the pitting potential to more positive values, i.e. decreases the pitting corrosion. The adsorption of the inhibitors on the iron surfaces can prevent the adsorption of Cl^- ion (which is responsible for pitting corrosion).

3.5. Electrochemical impedance spectroscopy

Nyquist plots of iron in uninhibited and inhibited 3.5% NaCl solution containing various concentrations of $SmCl_3$ are shown in Fig. 8. As can see from this figure, the Nyquist plots are not perfect semicircles as expected from the theory of EIS and this difference can be attributed to the frequency dispersion as a result of roughness and in homogeneity of the electrode surface. Increase in the diameters of the semicircles with the concentration of the additives indicates the increase in the protective properties of the iron surface. Thus, the capacitive semicircle is correlated with the dielectric properties and the thickness of barrier adsorbed film.

Impedance parameters, such as charge transfer resistance R_{ct}, which is equivalent to R_p, and the double layer capacitance C_{dl} derived from the Nyquist plots are given in Table 5 for iron in 3.5% NaCl solution in the presence and absence of the lanthanides. It is observed that the values of R_{ct} increase with increasing the concentration of the inhibitors and this in turn leads to a decrease in corrosion rate of iron. On the other hand, the values of C_{dl} decreased with increase in inhibitors concentration. This situation was a result of increasing surface coverage by the inhibitor, which led to an increase in % IE. The thickness of the protective layer, δ_{org}, was related to C_{dl} by the following equation [26,27]:

$$C_{d1} = \varepsilon_o \, \varepsilon_r / \delta_{org} \quad (8)$$

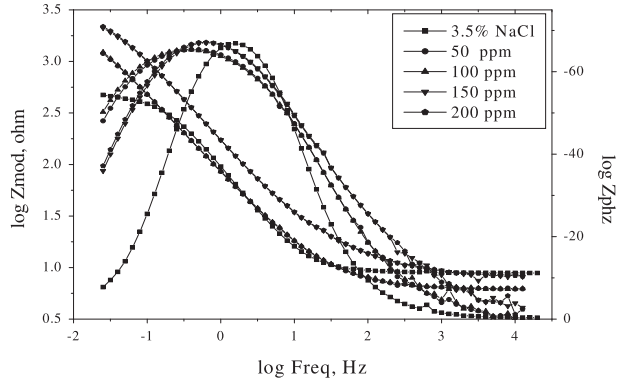

Fig. 9. The bode plots for corrosion of iron 3.5% NaCl in the absence and presence of different concentrations of $SmCl_3$ at 25°C.

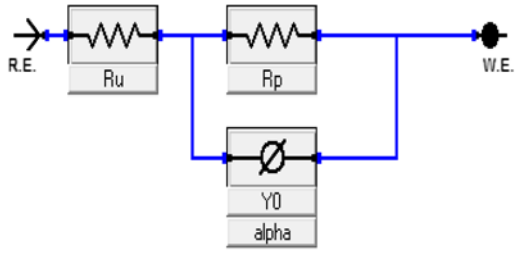

Fig. 10. An equivalent circuit used to fit Nyquist plots.

where ε_o is the vacuum dielectric constant and ε_r is the relative dielectric constant. The decrease in C_{dl} can result from a decrease in local dielectric constant and/or an increase in the thickness of the electric double layer [28], suggesting that lanthanide molecules function by adsorption at the metal/solution interface. Thus, the change in C_{dl} values was caused by the gradual replacement of water molecules by the adsorption of the lanthanide molecules on the metal surface, decreasing the extent of dissolution reaction [29].

Bode plots of iron in uninhibited and inhibited 3.5% NaCl solution containing various concentrations of $SmCl_3$ are shown in Fig. 9. The high frequency limit corresponds to the solution resistance $R_s(R)$, while the lower frequency limit represents the sum of $(R_s + R_{ct})$. The values of R_{ct} and R_s calculated from Nyquist and Bode plots are in good agreement. The impedance data are analyzed in terms of an equivalent circuit model (Fig. 10) which includes the solution resistance R_s or R_Ω and the double layer capacitance C_{dl} which is placed in parallel to the charge transfer resistance R_{ct} due to the charge transfer reaction.

The value of phase angle (θ) corresponding to the resistive behavior of R_s and $(R_s + R_t)$ tends towards 90°. The presence of one phase maximum at intermediate frequencies indicates the presence of one time constant corresponding to the impedance of the formed protective film.

In addition to the values of R_{ct} and C_{dl} calculated from EIS data, the values of the surface coverage (θ)

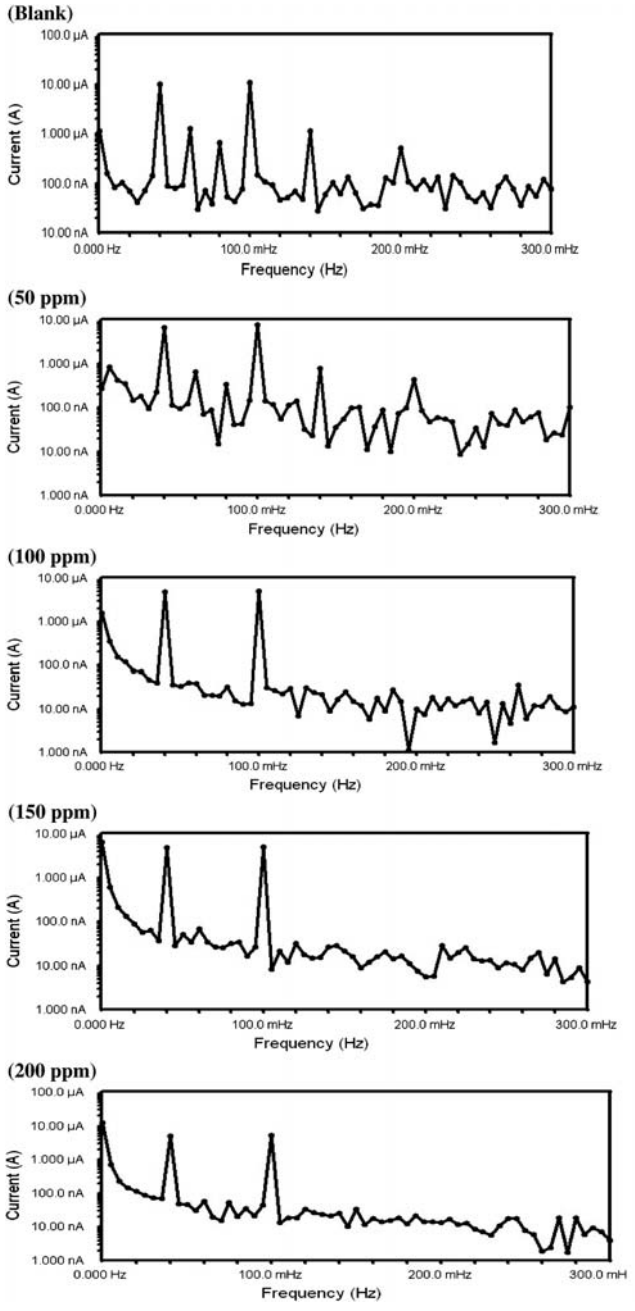

Fig. 11. Intermodulation spectrum for iron metal in 3.5% NaCl in the presence of 50–200 ppm of $SmCl_3$ at 25°C.

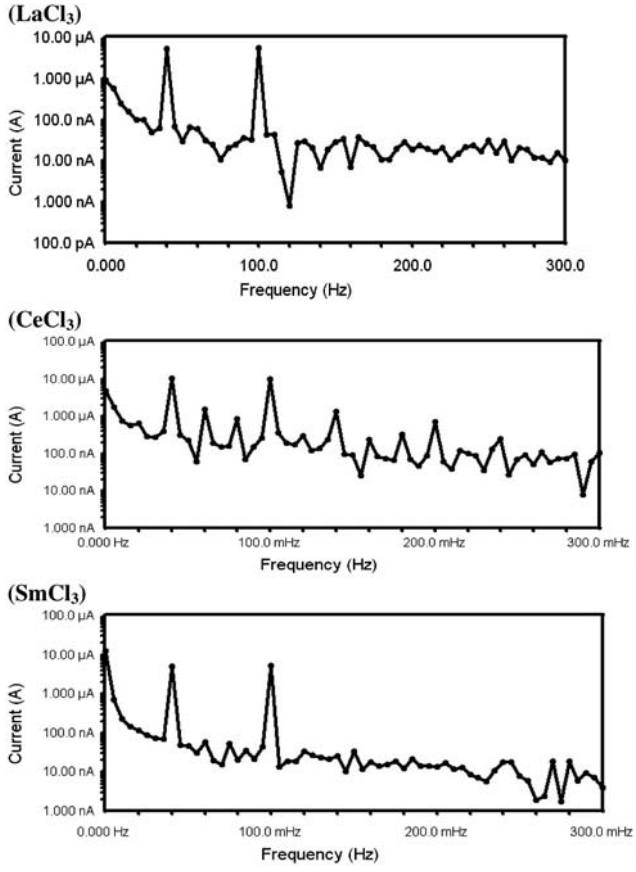

Fig. 12. Intermodulation spectrum for iron metal in 3.5% NaCl in the presence of 200 ppm of lanthanides chlorides compounds.

and the percentage inhibition ($\eta\%$) were calculated in presence and absence of lanthanides chlorides as shown in Table 5, from the following equations:

$$\eta\ (\%) = \theta \times 100 = [1 - (R_{ct}/R_{ct})] \times 100 \quad (9)$$

where $(R_{ct})_{free}$ and $(R_{ct})_{add}$ are charge transfer resistance in blank and in presence of additive, respectively.

From the data given in Table 5, the order of decreasing inhibition efficiency for the tested compounds is: $SmCl_3 > CeCl_3 > LaCl_3$.

Apparently, the results obtained from impedance technique give further support to the results predicted from potentiodynamic polarization techniques.

3.6. EFM technique

Results of EFM experiments are a spectrum of current response as function of frequency .The spectrum is called the "inter modulation spectrum" and an example is shown in Fig. 11. Fig. 12 shows intermodulation spectrum for iron metal in 3.5% NaCl in the presence of 200 ppm of lanthanides chlorides compounds. The harmonic and intermodulation peaks are clearly visible and are much larger than background noise .The two large peaks, with amplitudes of about 200 μA, are the response to the 2 and 5 Hz excitation frequencies. Those peaks between 1 and 20μA are the harmonic, sums, and differences of the two excitation frequencies. Analysis of these peaks at intermodulation frequencies can reveal the corrosion rate and Tafel parameters. It is important to note that between the peaks the current response is very small. The corrosion parameters, such as inhibition efficiency ($\eta\%$), corrosion current density ($\mu A\ cm^{-2}$), Tafel constants, and causality factors: CF-2 and CF-3, at different concentrations of lanthanides in 3.5% NaCl at 25℃ are presented in Table 6. It is observed that the corrosion current densities decreased by increase of the different concentrations of lanthanides chlorides. The CF indicated that the measured data are of good quality .The standard values for CF-2 and CF-3 are 2 and 3, respectively. The causality factor is calculated from the frequency spectrum of the current response. If the causality factors are approximately equal to the predicted values of 2 and 3, there is a causal relationship between the perturbation signal and the response signal. Then the data are assumed to be reliable [30]. When CF-2 and CF-3 are in the range 0–2 and 0–3, respectively, then the EFM data is valid. The deviation of causality factors from their ideal values might due to that the perturbation amplitude was too small or that the resolution of the frequency spectrum is not high enough also another possible explanation that the inhibitor is not performing very well [31].

3.7. Scanning electron microscopy (SEM) studies

The SEM micrographs of the specimen surface after 48 h of immersion in 3.5% NaCl solution in the absence and presence of different concentrations of $SmCl_3$ as corrosion inhibitor are shown in Fig. 13. In the blank micrograph, flakes showing corrosion products can be observed [32]. However, no pits or cracks can be seen in the micrographs. On the other

Table 6
Electrochemical parameters obtained by EFM technique for iron in 3.5% NaCl in the absence and presence of various concentrations of lanthanides chlorides at 25℃

Inh.	[Inh.] (ppm)	j_{corr} ($\mu A\ cm^{-2}$)	β_a ($mV\ dec^{-1}$)	β_c ($mV\ dec^{-1}$)	CF-2	CF-3	η (%)
	00	46.76	144	276	2.037	3.11	0.0
$LaCl_3$	50	18.10	90	105	1.721	2.874	61.3
	100	15.69	41	60	1.78	3.067	66.4
	150	13.46	81	159	1.716	2.879	71.2
	200	11.81	139	147	1.808	3.28	74.7
$CeCl_3$	50	14.07	37	53	1.89	2.954	69.9
	100	12.67	65	116	2.079	3.256	72.9
	150	11.27	117	128	2.866	1.977	75.9
	200	10.68	53	97	1.836	1.837	77.2
$SmCl_3$	50	13.35	88	193	1.847	2.786	71.5
	100	12.18	155	164	1.94	3.207	74.0
	150	11.15	140	153	2.814	2.73	76.2
	200	10.10	125	133	2.17	3.199	78.4

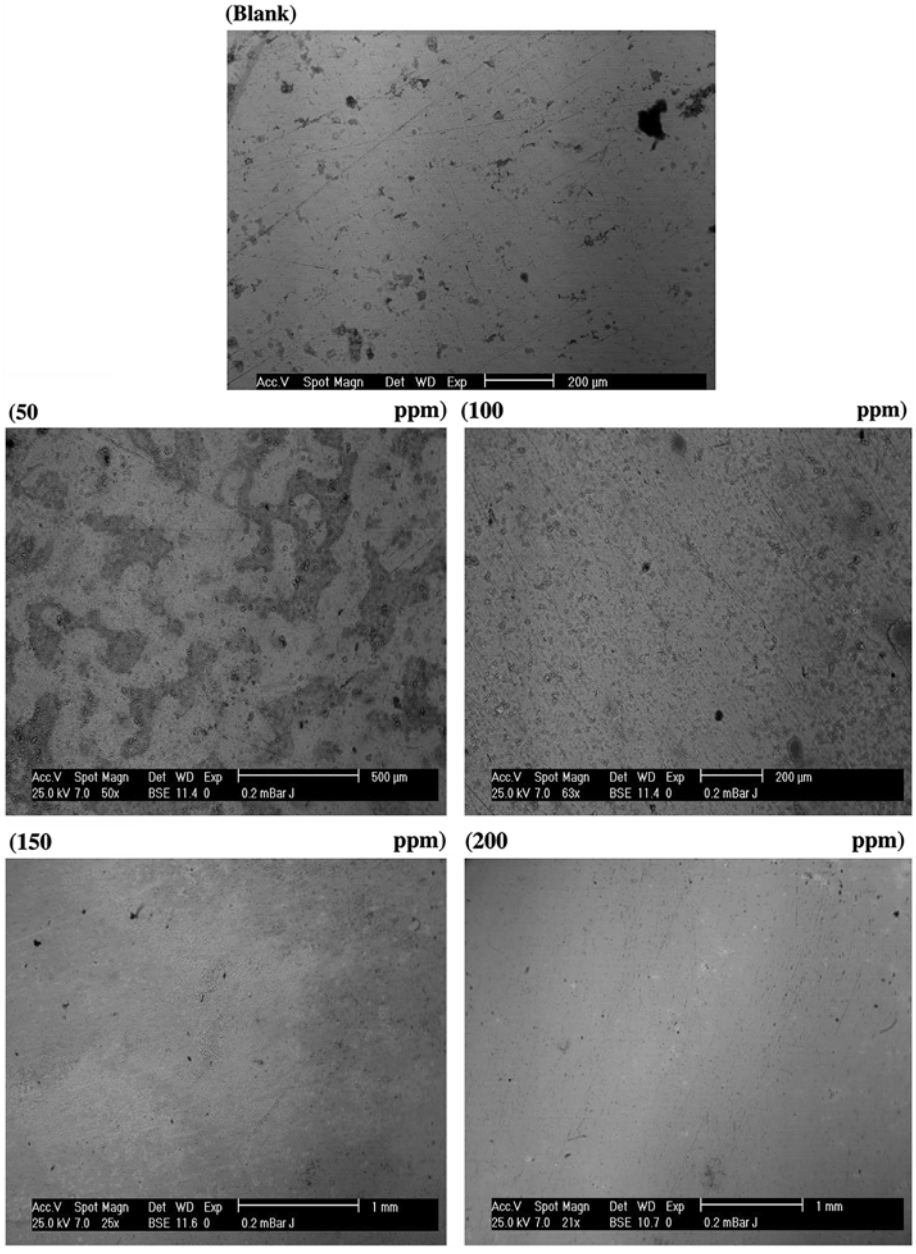

Fig. 13. SEM spectrum of iron before and after immersion for 48 h in 3.5%NaCl solution without and with different concentrations (50–200 ppm) of $SmCl_3$.

hand, for the alloy surface which was inhibited with different concentrations of $SmCl_3$ (50, 100, 150, and 200 ppm) for 48 h immersion, it can be seen that the flakes in the surface of specimens are reduced when compared with that of the micrograph of the blank. The specimen surface can be observed to be covered with a thin layer of the $SmCl_3$ molecules, which increases by increasing the concentration of the inhibitor ($SmCl_3$), giving protection against corrosion. Fig. 14 shows SEM micrographs of iron before and after immersion for 48 h in 3.5% NaCl solution with 200 ppm of lanthanides. The effect of the formation of thin film of lanthanides on the iron surface decreases in the following order: $SmCl_3 > CeCl_3 > LaCl_3$.

3.8. Electron dispersion X-Ray (EDX) studies

The EDX spectra were used to determine the elements present on the surface of the iron after 48 h of exposure to the uninhibited and inhibited 3.5% NaCl

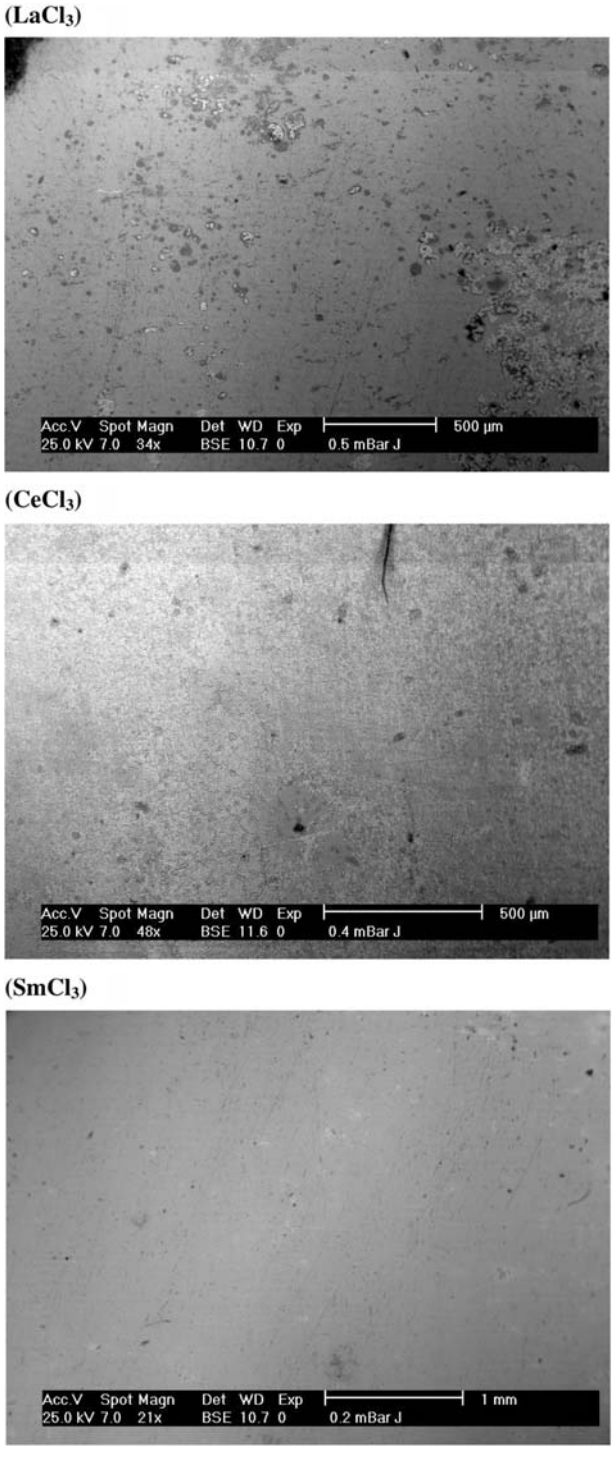

Fig. 14. SEM spectrum of iron before and after immersion for 48 h in 3.5%NaCl solution with 200 ppm of lanthanides chlorides.

solution. Fig. 15 (blank) shows the EDX analysis result on the composition of iron without the inhibitor treatment. The EDX analysis indicates that only Fe and Cl were detected. The EDX analysis of the iron in 3.5% NaCl in the presence of 50, 100, 150, and 200 ppm of $SmCl_3$, for example, the spectra show an additional line, demonstrating the existence of Sm and the height of this line increases by increasing the concentration of $SmCl_3$. Fig. 16 shows the EDX analysis of the three lanthanides at 200 ppm. This figure shows the presence of peaks related to La, Ce, and Sm, this revealed the presence of a protective film of lanthanides on iron surface. The height of the peak increases as follows: La < Ce < Sm and this parallel to the order of inhibition efficiency of these inhibitors.

3.9. Mechanism of inhibition

The obtained results by potentiodynamic polarization, EIS, EFM, SEM, and EDX techniques indicate that the extent of inhibition of lanthanides for corrosion of iron in 3.5% NaCl solution obeys the following order: $SmCl_3 > CeCl_3 > LaCl_3$. The inhibition efficiency values can be explained on the basis of formation of lanthanide oxides or hydroxides over cathodic sites and nodule formation. Blocking of cathodic sites by these nodules decreases the available cathodic current and, therefore, reduces the principal corrosion process of iron. This explanation is supported by the results of several authors [33].

The explanation of the precipitation mechanism of rare earth oxides and hydroxides is based on the hydrolysis reactions experienced by the rare earth cations as proposed by Baes and Mesmer [34].

$$xM^{y+} + yH_2O \rightarrow M_x(OH)_y^{(xy-y)} + yH^+ \quad (10)$$

This reaction explains why each solution starts at a different pH according to its concentration and its solubility constant (Table 7).

As the product of this reaction, a complex hydroxylate is obtained whose stoichiometry depends on the pH of the solution, so that the higher the pH, the more favored is the precipitation of $Ln(OH)_3$:

$$Ln^3 + 3H_2O \rightarrow Ln(OH)_3 + 3H^+ \quad (11)$$

The rare earth hydroxides formed do not possess amphoteric properties, which are stable in alkali solutions and dissolve in acid solutions. Consequently, the hydroxides will precipitate in those areas where pH is sufficiently alkaline to reach their solubility product.

The solubility of Sm^{3+}, Ce^{3+}, and La^{3+} cations is given according to Pourbaix by the following equilibrium [35]

$$2Sm^{3+} + 3H_2O = Sm_3O_2 + 6H^+$$

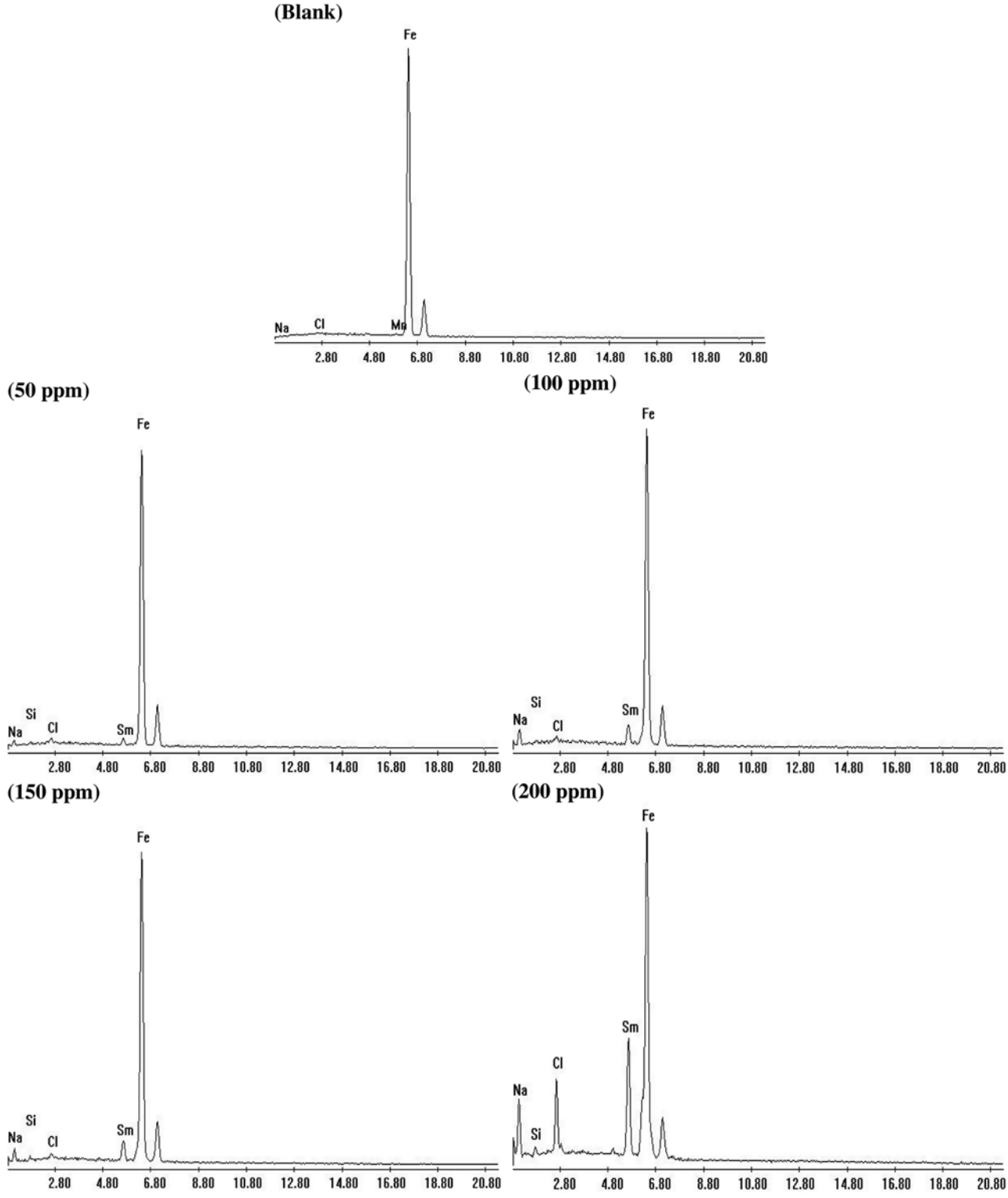

Fig. 15. EDX spectrum of iron before and after immersion for 48 h in 3.5%NaCl solution without and with different concentrations (50–200 ppm) of $SmCl_3$.

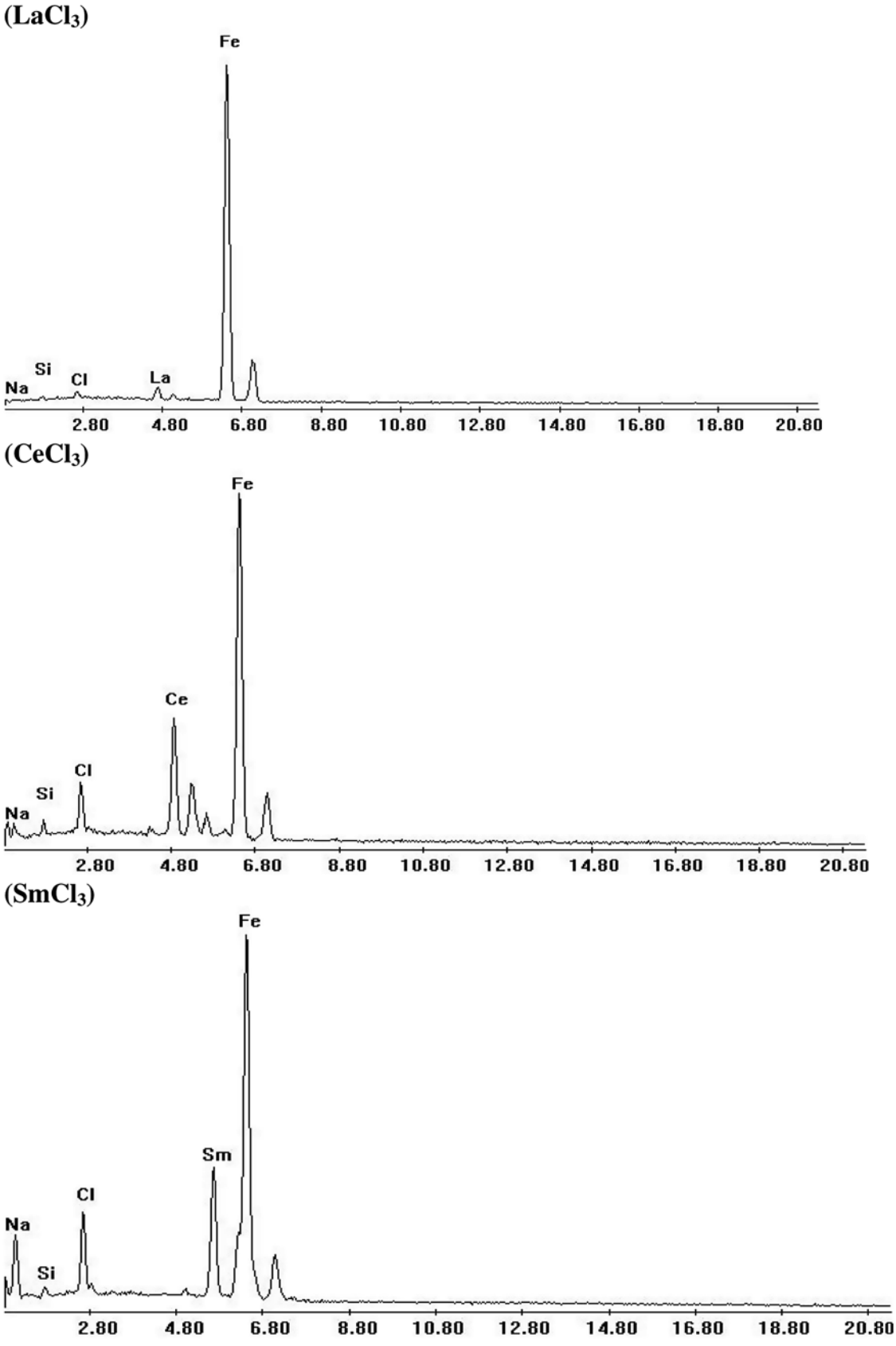

Fig. 16. EDX spectrum of iron before and after immersion for 48 h in 3.5% NaCl solution with 200 ppm of lanthanides chlorides.

Table 7
pH values From Sm ,Ce and La solutions according to the different concentrations

[inh.] (ppm)	pH		
	$SmCl_3$	$CeCl_3$	$LaCl_3$
50	6.12	6.08	5.69
100	6.2	6.02	5.88
150	6.24	6.05	5.95
200	6.59	6.1	5.96

$$\log(Sm^{3+}) = 21.10 - 3pH \quad (12)$$

$$2Ce^{3+} + 3H_2O = Ce_3O_2 + 6H^+$$

$$\log(Ce^{3+}) = 22.15 - 3pH \quad (13)$$

$$2\ La^{3+} + 3H_2O = La_3O_2 + 6H^+$$

$$\log(La^{3+}) = 23.02 - 3pH \quad (14)$$

Supposing that the cerium, samarium, and lanthanum cations hydrolyze to precipitate the species $La(OH)_3$, it is possible to calculate the critical pH at which their precipitation occurs. These pH values are lower than theoretical pH that was calculated, which was reached on the cathodic areas, and therefore, the precipitation of the rare earth hydroxides is thermodynamically favorable, whether it occurs with an exchange of two or four electrons.

For the same pH value, a greater concentration of $[Ln^{3+}]$ is needed for $La(OH)_3$ to precipitate than $Ce(OH)_3$ and than $Sm(OH)_3$. So, at the same pH the rate of formation of $Ln(OH)_3$ is decreased in the following order: $Sm(OH)_3 > Ce(OH)_3 > La(OH)_3$ which is parallel to their inhibition efficiency.

4. Conclusion

The corrosion studies of the iron were carried out at room temperature using seawater (3.5% NaCl), and the results indicated that lanthanides are effective corrosion inhibitor for iron in seawater. The studied inhibitors were observed to act as a mixed-type inhibitor, and EIS measurements clarified that the corrosion process was mainly controlled by charge transfer, and that no change in the corrosion mechanism occurred owing to the addition of inhibitor in seawater. The values of R_{ct} increased with the addition of inhibitor, while the capacitance values decreased, indicating the formation of a surface film. The surface study (by SEM) indicated the formation of thin film on the iron specimen immersed in seawater containing the lanthanides.

References

[1] T.J. Haley, Effect of surface preparation prior to cerium pretreatment, J. Pharm. Sci. 54 (1965) 633–635.
[2] P.J. Falconnet, The rare earth industry: a world of rapid change, J. Alloys Comp. 192 (1993) 114–118.
[3] S.R. Taylor, Abundance of chemical elements in the continental crust: A new table, Geochim. Cosmochim. Acta 28 (1964) 1273–1285.
[4] B.R.W, Hinton, L.Wilson, The corrosion inhibition of zinc with cerous chloride, Corros. Sci. 29 (1989) 967–985.
[5] N. Verma, W.R. Singh, S.K. Tiwari, R.N. Singh, Influence of minor additions of La, Ce and Nd on the corrosion behavior of aluminum bronze in sulphuric acid solution, Br. Corros. J. 25 (1990) 131–142.
[6] F. Czrewinski, W.W. Smeltzer, Oxidation of metals, Lanthanide compounds as environmentally-friendly corrosion inhibitors of aluminum alloys: a review 40 (1993) 503–522.
[7] H.S. Isaacs, A.J. Davenport, A. Shipley, Electrochemical response of steel to the presence of dissolved cerium, J. Electrochem. Soc. 138 (1991) 390–393.
[8] S.K. Mitra, S.K. Roy, S.K. Bose, Influence of superficial coating of CeO_2 on the oxidation behavior of AISI 304 stainless steel, Oxidation Metals 39 (1993) 221–229.
[9] S. Bernal, F.J. Botana, J.J. Calvino, M.A. Cauqui, M. Marcos, J.A. Perez, H. Vidal, in Proc. Lanthanide compounds as environmentally-friendly corrosion, Reunion Nac.de Materials, Oviedo, 1993, p. 258.
[10] S. Bernal, F.J. Botana, J.J. Calvino, M.A. Cauqui, M. Marcos, J.A. Perez, H. Vidal, in: Proc. Lanthanide compounds as environmentally-friendly corrosion inhibitors, Visualizer—Untitled 13th Int. Conf. Electron Microscopy, Parts, Francia, 1994 (1994) 1105–1112.
[11] S. Bernal, F.J. Botana, J.J. Calvino, MA. Cauqui, M. Marcos, J.A. Perez, H. Vidal, Lanthanide compounds as environmentally-friendly corrosion inhibitors, in: Proc. 2nd Int. Conf. on Elements, Helsinkii, Finlandia, 1994, p. 354.
[12] S. Bernal, F.J. Botana, J.J. Calvino, M.A. Cauqui, M. Marcos, J.A. Perez, Lanthanide compounds as environmentally-friendly corrosion inhibitors, in: Proc. 5th Elect. Methods in Corros. Research, Sesimbra, Portugal, 1994, p. 10.
[13] Y.C. Lu, M.B. Ives, Chemical treatment with cerium to improve the crevice corrosion resistance of austenitic stainless steels, Corros. Sci. 37 (1995) 145–155.

[14] S. Bernal, F.J. Botana, J.J. Calvino, M.A. Cauqui, M. Marcos, J.A. Perez, H. Vidal, Lanthanide salts as alternative corrosion inhibitors, J. Alloys Comp. 225 (1995) 638–641.
[15] K. Al-Muhanna, Corrosion behavior of different stainless steel alloys exposed to flowing fresh seawater by electrochemical impedance spectroscopy, Desalin. Water Treat. 29 (2011) 227–235.
[16] N. Larche, P. Dezerville, Review of material selection and corrosion in seawater reverse osmosis desalination plants, Desalin. Water Treat. 31 (2011) 121–133.
[17] A.U. Malik, I. Andijani, M. Mobin, S. Al-Fozan, F. Al-Muaili, M. Al-Hajiri, An overview of the localized corrosion problems—some recent case studies, Desalin. Water Treat. 20 (2011) 22–35.
[18] F. Bentiss, M. Lebrini, M. Lagrenee, Thermodynamic characterization of metal dissolution and inhibitor adsorption processes in mild steel/2,5-bis(n-thienyl)-1,3,4-thiadiazoles/ hydrochloric acid system, Corros. Sci. 472 (2005) 915–918.
[19] E.S. Ferreira, C. Giancomelli, F.C. Giacomelli, A. Spinelli, Evaluation of the inhibitor effect of L-ascorbic acid on the corrosion of mild steel, Mater. Chem. Phys. 83 (2004) 129–134.
[20] O. Olivares, N.V. Likhanova, B. Gomez, J. Navarrete, M.E. Llanos-Serrano, E. Arce, J.M. Hallen, Electrochemical and XPS studies of decylamides of Î±-amino acids adsorption on carbon steel in acidic environment, Appl. Surf. Sci. 252 (2006) 2894–2909.
[21] K.F. Khaled, The inhibition of benzimidazole derivatives on corrosion of iron in 1 M HCl solutions, Electrochim. Acta 48 (2003) 2493–2503.
[22] E.A. Noor, A.H. Al-Moubaraki, Thermodynamic study of metal corrosion and inhibitor adsorption processes in mild steel/1-methyl-4[4′(-X)-styryl pyridinium iodides/ hydrochloric acid systems, Mater. Chem. Phys. 110 (2008) 145–154.
[23] A.K. Singh, M.A. Quraishi, Effect of Cefazolin on the corrosion of mild steel in HCl solution, Corros. Sci. 52 (2010) 156–164.
[24] Y.A. El-Awady, A.I. Ahmed, The effect of some ethoxylated fatty acids on corrosion, J. Ind. Chem. 24 (1985) 601–613.
[25] G.K. Gomma, M.H. Wahdan, Effect of azole compounds on corrosion of copper in acid medium, Mater. Chem. Phys 39 (1995) 209–213.
[26] J.A. Dean, Lange's Handbook of Chemistry, second ed., New York, NY, McGraw-Hill, 1973, p. 148.
[27] F. Bentiss, M. Lagrenee, B. Elmehdi, B. Mernari, M. Traisnel, H. Vezin, Electrochemical and quantum chemical sudies of 3,5-di(n-Tolyl)-4-amino-1,2,4-triazole adsorption on mild steel in acidic media, Corrosion 58 (2002) 399–407.
[28] E. McCafferty, N. Hackerman, Double layer capacitance of iron and corrosion inhibition with polymethylene diamines, J. Electrochem. Soc. 119 (1972) 146–154.
[29] S. Muralidharan, K.L. Phani, S. PItchumani, S. Ravichandran, S.V. Iyer, Polyamino-benzoquinone polymers: a new class of corrosion inhibitors for mild steel, J. Electrochem. Soc. 142 (1994) 1478–1483.
[30] M. Lagrenee, B. Mernari, B. Bouanis, M. Traisnel, F. Bentiss, Study of the mechanism and inhibiting efficiency of 3,5-bis (4-methylthiophenyl)-4H-1,2,4-triazole on mild steel corrosion in acidic media, Corros. Sci. 44 (2002) 573–588.
[31] R.W. Bosch, J. Hubrecht, W.F. Bogaerts, B.C. Syrett, Performance and non-destructive. Evaluation group, Corrosion 57 (2001) 60–70.
[32] S.S. Abdel-Rehim, K.F. Khaled, N.S. Abd-Elshafi, Electrochemical frequency modulation as a new technique for monitoring corrosion inhibition of iron in acid media by new thiourea derivative, Electrochim. Acta 51 (2006) 3269–3277.
[33] R. Rosliza, H.B. Senin, W.B. Wan Nik, Study on the effect of vanillin on the corrosion inhibition of aluminum alloy, Colloids Surf. A. 312 (2008) 185–189.
[34] C.F. Baes, R.E. Mesmer, in: Proceedings of the First International Symposium on Chemical, The Hydrolysis of Cations, John Wiley and Sons, New York, NY, 1976, p. 489.
[35] M. Pourbaix, Atlas of Electrochemical Equilibria in Aqueous Solutions, Pergamon Press, London, 1966, p. 183.